

# Facile Immobilization of Ag Nanocluster on Nanofibrous Membrane for Oil/Water Separation

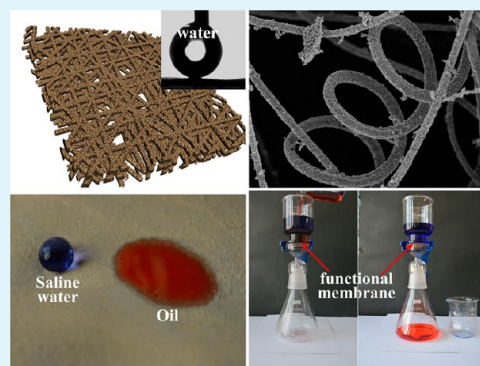
Xiong Li, Min Wang, Ce Wang, Cheng Cheng, and Xuefen Wang\*

State Key Laboratory for Modification of Chemical Fibers and Polymer Materials, Donghua University, Shanghai 201620, People's Republic of China

## S Supporting Information

**ABSTRACT:** Superhydrophobic and superoleophilic electrospun nanofibrous membranes exhibiting excellent oil/water separation performance were green fabricated by a facile route combining the amination of electrospun polyacrylonitrile (APAN) nanofibers and immobilization of a Ag nanocluster with an electroless plating technique, followed by *n*-hexadecyl mercaptan (RSH) surface modification. By introducing the hierarchically rough structures and low surface energy, the pristine superhydrophilic APAN nanofibrous membranes could be endowed with a superhydrophobicity with water contact angle of  $171.1 \pm 2.3^\circ$ , a superoleophilicity with oil contact angle of  $0^\circ$  and a self-cleaning surface arising from the extremely low water contact angle hysteresis ( $3.0 \pm 0.6^\circ$ ) and a low water-adhesion property. Surface morphology studies have indicated that the selective wettability of the resultant membranes could be manipulated by tuning the electroless plating time as well as the hierarchical structures. More importantly, the extremely high liquid entry pressure of water (LEPw,  $175 \pm 3$  kPa) and the robust fiber morphology of the APAN immobilized Ag nanocluster endowed the as-prepared membranes with excellent separation capability and stability for oil/water separation by a solely gravity-driven process. The resultant membranes exhibited remarkable separation efficiency in both hyper-saline environment and broad pH range conditions, as well as excellent recyclability, which would make them a promising candidate for industrial oil-contaminated water treatments and marine spilt oil cleanup, and provided a new prospect to achieve functional nanofibrous membranes for oil/water separation.

**KEYWORDS:** electrospinning, superhydrophobicity, nanocluster, immobilization, oil/water separation



## INTRODUCTION

Owing to the increasing industrial oily wastewater accompanying the frequent oil spill accidents such as the catastrophic Deepwater Horizon oil spill in the Gulf of Mexico,<sup>1,2</sup> it is of vital importance to develop novel technologies to achieve oil/water separation efficiently.<sup>3–6</sup> Conventional techniques such as skimming, ultrasonic separation, air flotation, gravity processing, membrane filtration and coagulation–floculation are often limited by the low separation efficiency, high energy-cost, secondary pollution and complex separation devices, etc.<sup>7–10</sup> Therefore, efficient, environmentally friendly and cost-effective novel functional materials with excellent stability in complex practical environments for oil/water separation, especially solely gravity-driven separation membranes, are urgently desired.

In consideration of the interfacial process of oil/water separation, it is an effective and facile strategy to design novel materials by taking advantage of the bio-inspired special wettability, which is controlled by the surface chemical composition and geometrical structure.<sup>11–13</sup> According to the Wenzel and Cassie–Baxter model,<sup>14,15</sup> the introduction of an appropriate multiscale roughness could make a hydrophobic surface more hydrophobic or even superhydrophobic due to

the air pockets to be entrapped beneath the water droplet as a repulsive cushion, whereas an oleophilic surface becomes more oleophilic or even superoleophilic due to the capillary effect.<sup>16,17</sup> Thus, a membrane surface that simultaneously exhibited superhydrophobic and superoleophilic could be obtained by the incorporation of proper rough topography and low surface energy.

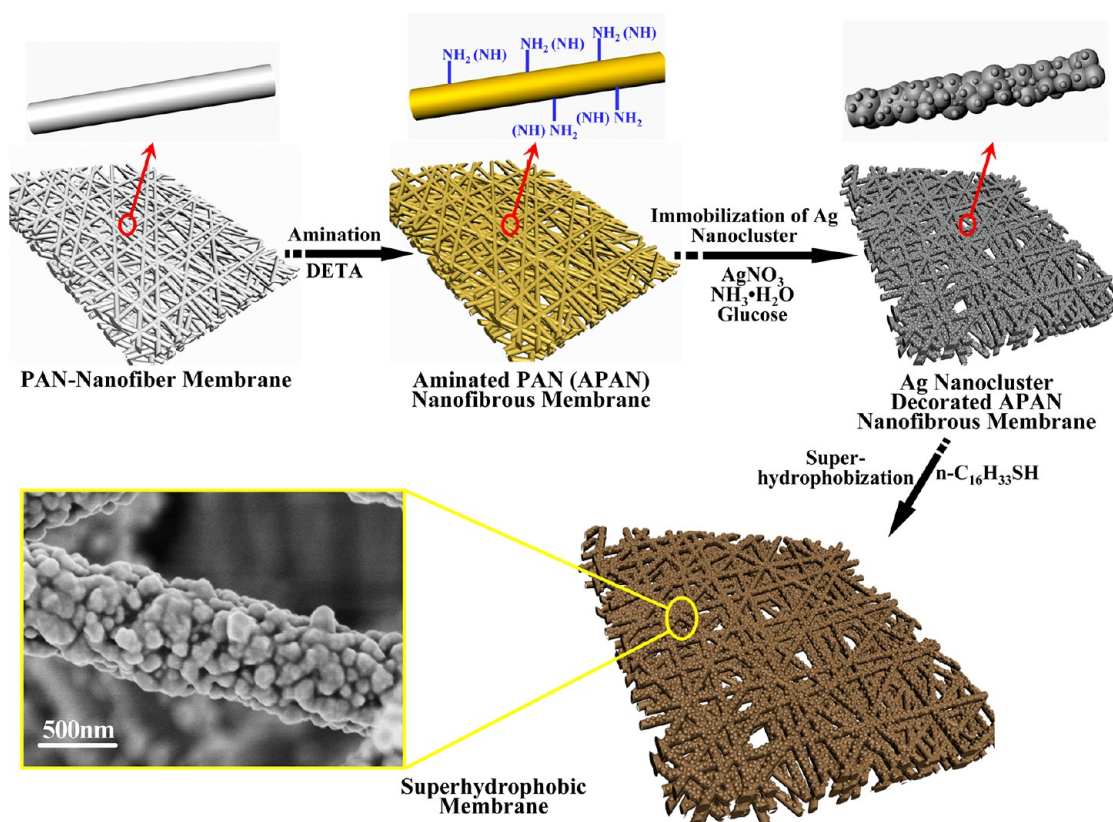
Since the first report of a polytetrafluoroethylene (PTFE) coated mesh with superhydrophobicity and superoleophilicity for oil/water separation by Feng et al.,<sup>18</sup> various approaches have been utilized for the fabrication of superhydrophobic membranes, including self-assembly, chemical etching, electrochemical process, chemical vapor deposition, plasma treatment and lithography, etc.<sup>19–24</sup> Nevertheless, there still exist lots of limitations for large-scale fabrication of such functional membranes for practical applications, due to the costly, tedious and toxic fabrication procedures like fluorochemicals modification, low stability and flexibility in harsh practical environments and poor recyclability. It is noteworthy that the

Received: June 12, 2014

Accepted: August 12, 2014

Published: August 12, 2014

Scheme 1. Illustration for the Fabrication Procedure of Superhydrophobic Aminated PAN (APAN) Nanofibrous Membranes with Immobilized Ag Nanocluster



versatile and effective electrospinning technique has provided an ideal strategy for the construction of superhydrophobic nanofibrous membranes with highly controllable surface compositions and multiscale structures.<sup>25–28</sup> Typically, polystyrene (PS) with a low surface energy has been widely used to electrospin superhydrophobic fibrous mats for oil adsorption.<sup>29–31</sup> However, the inherent drawbacks of these functional membranes including weak stability in extreme environments, poor mechanical properties and antiwetting property from water pressure have been the primary obstacles for the practical applications, especially there is little investigation known about the use of superhydrophobic electrospun membranes for the solely gravity-driven oil/water separation. Recently, Ding et al.<sup>32,33</sup> demonstrated the fabrication of hybrid functional oil/water separation membranes with controllable wettability by combining the advantages of electrospun nanofibers with surface modification. Encouraging results were obtained from an in situ polymerized fluorinated polybenzoxazine functional layer that incorporated silica nanoparticles covered on nanofibers surfaces, in spite of the complex fabrication procedures and potential toxicity of fluorochemicals.

Significantly, immobilization of various nanoparticles onto complex two (2D) or three (3D) dimensional macroscopic surfaces is an important issue for nanotechnology,<sup>34,35</sup> which could provide a simple strategy to construct hierarchical roughness on the target surfaces. In this regard, a green and environmentally friendly electroless plating technique was often considered to construct the hierarchically rough structure that resulted from the silver nanoparticles immobilized on the various substrate surfaces.<sup>36,37</sup> Herein, we describe a new type of superhydrophobic and superoleophilic electrospun nano-

fibrous membranes with excellent oil/water separation performance via a facile and environmentally friendly route, which combined the amination of PAN (APAN) nanofibrous scaffold and the immobilization of Ag nanocluster with an electroless plating technique, followed by *n*-hexadecyl mercaptan (RSH) surface modification (as shown in Scheme 1). Wherein, Ag nanoclusters generated from the in situ reduction of silver ammonia solution by glucose were immobilized firmly and compactly on the surface of APAN nanofibers through the abundant amine and imine groups, and long chain thiols were easily bound to Ag nanoclusters firmly through Ag–S bonds. The separation capability of the as-prepared superhydrophobic membrane was evaluated by the liquid entry pressure of water (LEPW) for the first time. Furthermore, the robustness of the immobilized Ag nanocluster, separation stability in complex practical environments and recyclability were also demonstrated.

## EXPERIMENTAL SECTION

**Materials.** Polyacrylonitrile (PAN, with a weight-average molecular weight of 136 000 g/mol) was purchased directly from Shanghai Jinshan Co., Ltd. (China). *N,N'*-Dimethylformamide (DMF), diethylenetriamine (DETA), sodium carbonate ( $\text{Na}_2\text{CO}_3$ ), silver nitrate ( $\text{AgNO}_3$ ), ammonia solution ( $\text{NH}_3\cdot\text{H}_2\text{O}$ , 25%) and absolute ethanol were kindly supplied by Shanghai Lingfeng Chemical Reagent Co., Ltd. (China). Polyvinylpyrrolidone (PVP), glucose, *n*-hexadecyl mercaptan ( $n\text{-C}_{16}\text{H}_{33}\text{SH}$  (RSH)), 1,2-dibromoethane (EDB), methyl blue and Sudan III (85%) were purchased from Sigma-Aldrich. All chemicals were of analytical grade and were used as received without further purification.

**Electrospinning Details.** Typically, PAN was dissolved in DMF by mild stirring in an oil bath ( $\sim 50^\circ\text{C}$ ) for 24 h to obtain a 10 wt % homogeneous transparent solution. About 5 mL of the PAN/DMF



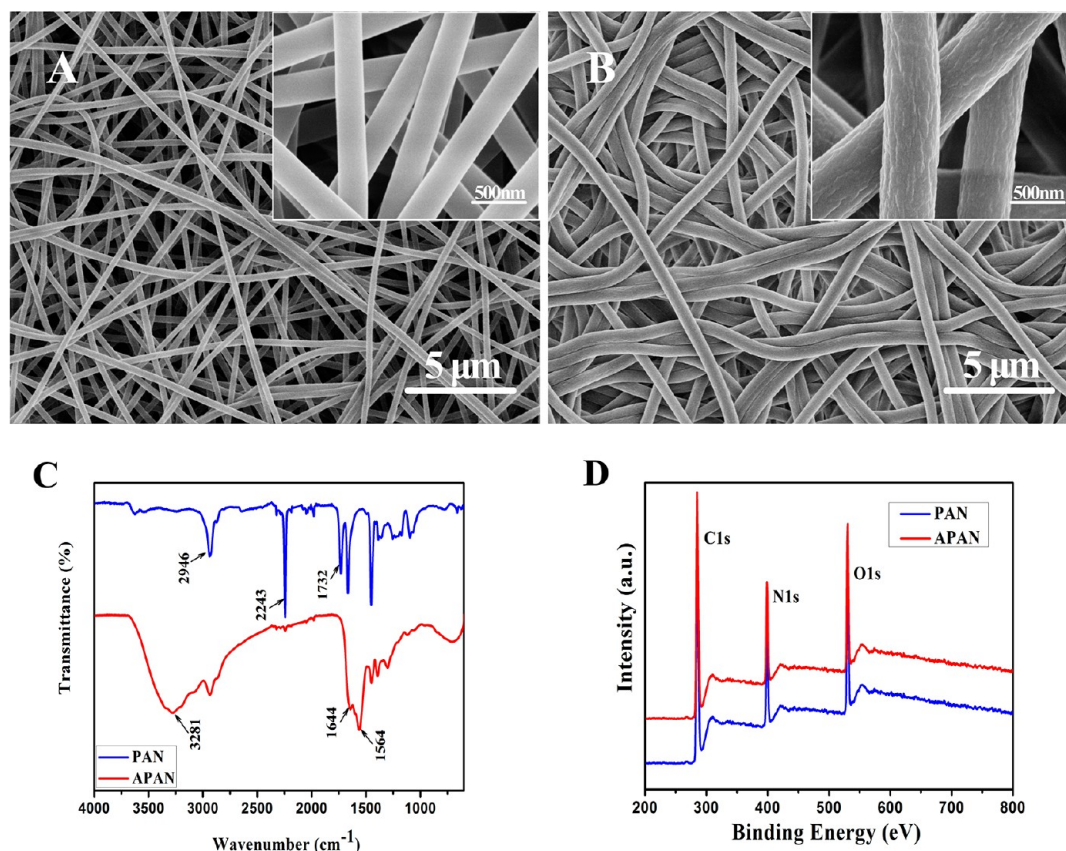


**Figure 1.** FE-SEM images of (A) PAN and (B) APAN nanofibrous membrane. (C) FT-IR spectra and (D) XPS wide-scan spectra of PAN and APAN membranes.

solution was placed in a 5 mL syringe equipped with a blunt metal needle of 0.37 mm inner diameter. The syringe was placed in a syringe pump that maintained a solution feeding rate of 1 mL/h. A grounded metallic rotating roller covered with a piece of aluminum foil was used as collector, which rotated at 500 rpm. The distance between the needle tip and collector was 15 cm, and the voltage was set at 25 kV. The relevant temperature and humidity were  $25 \pm 5$  °C and  $50 \pm 2\%$ , respectively. The obtained electrospun PAN nanofibrous scaffolds were dried in a vacuum oven at 60 °C for 12 h to remove the residual solvent.

#### Fabrication of Aminated PAN (APAN) Nanofibrous Mats.

The detailed methods and procedures for the preparation of aminated PAN nanofibers with amine and imine groups on the surfaces were described elsewhere.<sup>38</sup> In brief, four pieces of PAN nanofibrous mats ( $10 \times 10$  cm) were immersed in a 1000 mL closed reaction vessel containing 800 g of 25% (w/w) diethylenetriamine (DETA) solution and 6 g of sodium carbonate (catalyst); the reaction was allowed to proceed at 92 °C with  $N_2$  gas passing through the reaction mixture for 2 h for the amination of PAN nanofibers. Afterward, the membranes were separated from the solution when the vessel was cooled down to ambient temperature, thoroughly rinsed with deionized (DI) water until neutral and dried in a vacuum oven at 50 °C overnight.

**Immobilization of Ag Nanocluster and Superhydrophobization.** Immobilization of a Ag nanocluster on APAN nanofibrous membranes was fabricated by the electroless plating technique in a silver plating bath that was known as the silver mirror reaction. Ammoniacal silver nitrate solution was prepared by adding ammonia dropwise into the 1 wt %  $AgNO_3(aq)$  until the pH was controlled at 11, while the solutions became transparent. Then, the APAN membranes were immersed into the above solutions and kept mechanical shaking for 6 h in a shaking bath. The  $[Ag(NH_3)_2]^+$  ions were absorbed on the surface of nanofibers by the amine and imine groups. Subsequently, the same volume of 2 wt % glucose solution (including 0.04 wt % absolute ethanol and PVP to maintain

the stability of the plating bath) serving as a reducing agent was added slowly into the above mixture, and the electroless plating was allowed to continue from 30 to 100 min at room temperature. After the immobilization process, the membranes were separated from the plating bath, thoroughly rinsed with DI water and dried in a vacuum oven at 40 °C for 6 h.

The superhydrophobization process was conducted by immersing the Ag nanocluster decorated APAN nanofibrous membranes in an ethanol solution of 10 mM *n*-hexadecyl mercaptan (RSH) for 1 h, and then rinsed with a copious amount of absolute ethanol and dried in an oven at 50 °C for 2 h. The obtained samples will be denoted as APAN-Ag-SR-*x*, where *x* stands for the different electroless plating times.

**Characterizations.** The surface morphology of the sample was investigated by field emission scanning electron microscopy (FE-SEM, SU8000, Hitachi, Japan). The surface chemical compositions of the samples were measured by a Nicolet 8700 FT-IR spectrometer in the range of 650–4000  $cm^{-1}$  (attenuated total reflectance mode, Thermometer, USA) and X-ray photoelectron spectroscopy (XPS) (Kratos Axis UltraDLD spectrometer, Kratos Analytical-A Shimadzu Group Company) with monochromatic Al  $K\alpha$  radiation as the excitation and an X-ray power of 75 W. The wettability of the surface was performed by a dynamic contact angle testing instrument (OCA40, Dataphysics, Germany) equipped with a dynamic image capture camera. Average static water contact angle (WCA, 3  $\mu L$ ), oil contact angle (OCA, 3  $\mu L$ ) and water contact angle hysteresis (WCAH, 5  $\mu L$ , calculated from the difference between the advancing contact angle and the receding contact angle) were obtained by measuring the same sample at five different positions. The porosity of the membrane is defined as the volume of the pores divided by the total volume of the membrane, which was determined by a gravimetric method in this study.<sup>39</sup>

Liquid entry pressure of water (LEP<sub>w</sub>, mainly described in the field of membrane distillation) is commonly characterized as the ability of the membrane to hinder any liquid water penetrating into membrane

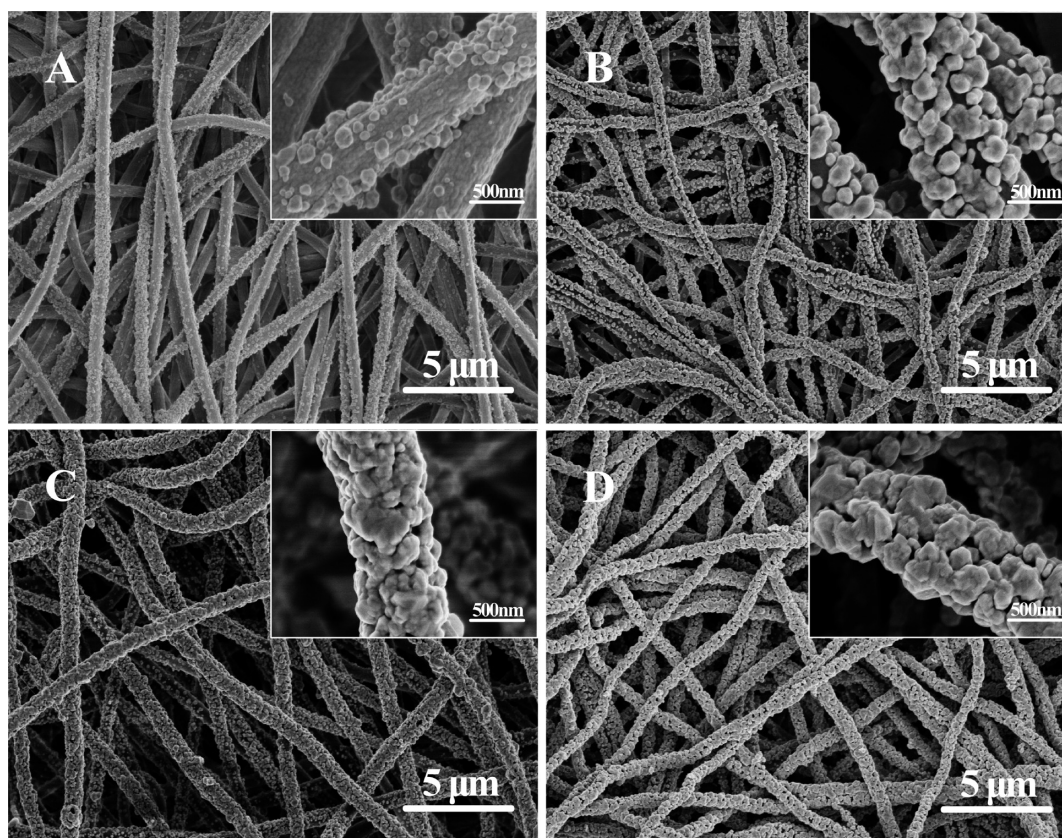


**Figure 2.** FE-SEM images of (A) APAN-Ag-SR-30, (B) APAN-Ag-SR-40, (C) APAN-Ag-SR-50 and (D) APAN-Ag-SR-60.

pores,<sup>39</sup> which can be used to assess the separation capability of the as-prepared superhydrophobic samples. A homemade experimental apparatus schematized in the Supporting Information (Figure S1)<sup>40</sup> was used for LEPw measurements. The dry APAN-Ag-SR-*x* nanofibrous sample with an effective area of 0.95 cm<sup>2</sup> was placed into the measuring cell and the reservoir was filled with DI water. By means of a gas cylinder that was filled with nitrogen, a slight pressure was raised stepwise with 0.005 bar and each pressure was maintained for 10 min in the process of the degasification of the permeate side and the LEPw test. The minimum applied pressure that resulted in a continuous flux was regarded as the LEPw value. The measurements were carried out thrice using three different membrane samples made under the same condition. The results were averaged to obtain the final LEPw value.

**Oil/Water Separation.** The as-prepared APAN-Ag-SR-*x* nanofibrous membrane was fixed between a glass funnel and a conical flask with an effective separation area of 12.6 cm<sup>2</sup>. A mixture of 100 mL of oil (1,2-dibromoethane (EDB)) colored with Sudan III and 100 mL of water colored with methyl blue was poured into the upper glass vessel and the separation was achieved, driven by gravity. Then the separated oil and water were collected with the conical flask and the glass vessel, respectively.

## RESULTS AND DISCUSSION

### Surface Modification of PAN Nanofibrous Scaffold.

Development of a facile, environmentally friendly and versatile strategy for surface modification of complex 2D or 3D macroscopic surfaces has gained substantial attention, which could endow the surfaces with sufficient “anchoring sites” for metal ions or nanoparticles to realize the effective immobilization process through noncovalent interactions or covalent bonding.<sup>34,35</sup> Herein, an aminated PAN (APAN) nanofibrous scaffold obtained by the graft of diethylenetriamine (DETA) on PAN nanofibers surfaces with abundant amine and imine

groups could provide sufficient chemisorption sites for silver ions to promote the electroless plating of silver. The representative FE-SEM image of electrospun PAN and APAN nanofibers shown in Figure 1A,B exhibited a randomly oriented 3D nonwoven scaffold with an average diameter of 300 and 550 nm, respectively. The obvious increment of APAN fiber diameter was attributed to the expansion of PAN nanofibers during the surface modification reaction. Significantly, close observation shows that the surfaces of APAN nanofibers became more rugged than that of PAN, probably ascribed to the graft of DETA on the nanofiber surface.<sup>41</sup>

The graft of DETA on PAN nanofibers surfaces can be confirmed from FT-IR spectral analysis (Figure 1C). The peaks around 2946 cm<sup>-1</sup> (CH stretching vibration in CH, CH<sub>2</sub> and CH<sub>3</sub> groups), 2243 cm<sup>-1</sup> (C≡N stretching) and 1732 cm<sup>-1</sup> (C=O stretching) of PAN samples almost completely disappeared and exhibited a new strong broad band with the peak at 3281 cm<sup>-1</sup>, which corresponds to the overlapping bands of both OH and NH groups after amination. Additionally, the peaks that appeared at 1644 and 1564 cm<sup>-1</sup> were assigned to the stretching vibration band of the C=O group in amide and the bending vibration band of N—H group in amine, respectively, indicating the graft of DETA on PAN, successfully as proposed (as shown in the Supporting Information, Scheme S1).<sup>42,43</sup> Furthermore, the typical X-ray photoelectron spectroscopy (XPS) analysis could also be used to further investigate the change of surface chemical composition of PAN and APAN nanofibers. As can be seen from Figure 1D, a one peak shape without binding energy change from the atoms of C, N and O has been detected, and exhibited some change in peak intensity due to the abundant amine and imine groups grafted on the PAN surface. Furthermore, the atom molar ratio



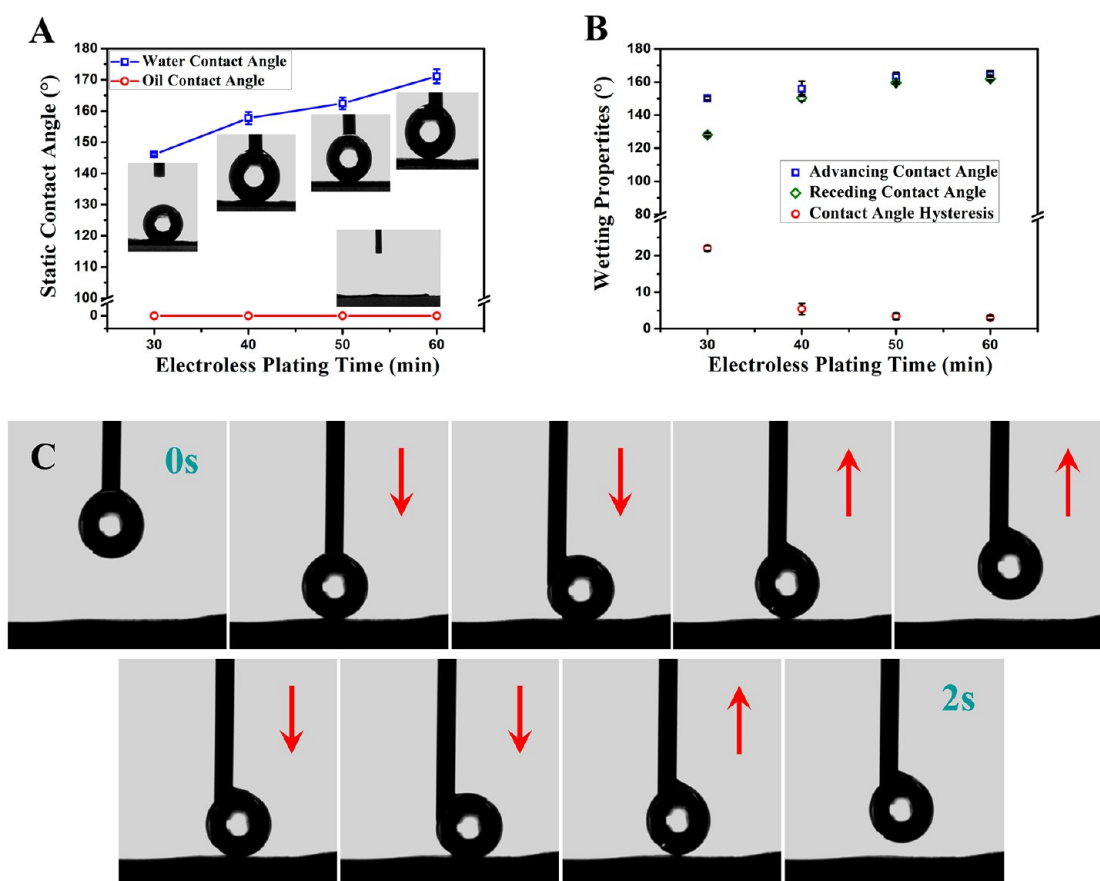


**Figure 3.** Surface wetting properties measured on the fabricated superhydrophobic membranes. (A) Static contact angles and (B) contact angle hysteresis variation from the different electroless plating time; (C) photographs of the dynamic water-adhesion behavior on the APAN-Ag-SR-50 surface within 2 s.

of N/C increased from 0.217 of PAN to 0.228 of APAN nanofibrous membranes (see the Supporting Information, Table S1). The N 1s core-level XPS spectra of PAN could be curve-fitted by only one peak at 398.6 eV for the nitrogen from the CN group, whereas that of APAN could be assigned to peaks at the binding energy of 398.6 and 399.9 eV for the nitrogen from the CN and NH<sub>2</sub> or NH groups, respectively (see the Supporting Information, Figure S2),<sup>42</sup> which further proved the introduction of DETA onto the surface of PAN nanofibers.

**Surface Morphology of APAN-Ag-SR.** Inspired by the special wettability of biological organisms from nature, the cooperation of their unique micro/nanoscale hierarchical surface structures and low surface energy is thought to be the contributing factor for the superhydrophobicity. It is noteworthy that a hierarchical structure is commonly recognized as the strategic factor for superhydrophobization due to the air pockets to be entrapped underneath the water droplet as a repulsive cushion.<sup>16,17</sup> Herein, an appropriate multiscale roughness was successfully constructed through the immobilization of the Ag nanocluster on the APAN nanofibers surfaces. The representative FE-SEM images of as-prepared APAN-Ag-SR shown in Figure 2A–D revealed that the morphology of modified APAN nanofibrous membranes was remarkably changed. It is clearly shown that only a small number of Ag nanoparticles (50–200 nm) were immobilized on the nanofibers surfaces during the early stage of electroless plating (30 min). With the extension of the electroless plating time to 40

min, the Ag nanocluster was gradually formed on the nanofibers, whereas it exhibited an unconsolidated morphology as shown in Figure 2B. With further extension of the electroless plating time to 50 min, the density of the Ag nanocluster increased and an extraordinarily compact enveloping morphology was observed (Figure 2C). When the electroless plating time was further increased to 60 min, the layer of the Ag nanocluster exhibited was much thicker and adhesions among the adjacent fibers were gradually generated (Figure 2D), which will reduce the porosity of the APAN-Ag-SR-60 membrane (as compared to the APAN-Ag-SR-30 sample with a high porosity of 90.5%, that of APAN-Ag-SR-60 membrane was decreased to 60.2%, see the Supporting Information, Table S2) and further affect the separation efficiency (permeate flux). Plenty of adhesions were clearly visible with the prolonged electroless plating time from 70 to 100 min (see the Supporting Information, Figure S3). Consequently, the combination of APAN nanofibers with immobilized the Ag nanocluster constructed the surface hierarchical roughness.

XPS was employed to confirm the surface chemical compositions of APAN-Ag and APAN-Ag-SR (see the Supporting Information, Figure S4). A strong signal of Ag at a binding energy (BE) of about 370 eV demonstrated the immobilization of the Ag nanocluster on APAN surfaces successfully. Meanwhile, the Ag 3d core-level spectrum could be curve-fitted by the Ag 3d<sub>5/2</sub> peak at a BE of 368.0 eV and the Ag 3d<sub>3/2</sub> peak at a BE of 374.0 eV, which were attributed to the Ag<sup>0</sup> species.<sup>37</sup> Additionally, the appearance of S 2p and C 1s

indicated the presence of thiol from APAN-Ag-SR. Wherein, the curve-fitted S 2p core-level spectrum exhibited two overlapping peaks centered at 162.3 eV, corresponding to the chemical bond of sulfur–silver, and the curve-fitted C 1s core-level spectrum contained one strong peak at a BE of 284.8 eV for the alkane group of thiol.<sup>44</sup> These XPS information fully confirmed the construction of multiscaled APAN-Ag-SR membranes successfully.

**Surface Wettability.** The wetting properties of water and oil (1,2-dibromoethane (EDB)) on the APAN-Ag-SR membranes were characterized comprehensively. As shown in Figure 3A, a superhydrophilic surface of APAN nanofibrous membrane showed a considerable transition in wetting behavior after surface modification. The static WCAs of APAN-Ag-SR-30, APAN-Ag-SR-40, APAN-Ag-SR-50 and APAN-Ag-SR-60 were  $146.1 \pm 0.5^\circ$ ,  $157.7 \pm 2.1^\circ$ ,  $162.4 \pm 1.9^\circ$  and  $171.1 \pm 2.3^\circ$ , respectively, indicating a remarkable increment of WCA toward the increasing electroless plating time due to the surface geometry effect.<sup>11–13</sup> Wherein, the insufficient immobilization of Ag nanoparticles on the APAN nanofiber surface resulted in the minimum WCA of APAN-Ag-SR-30, whereas the superhydrophobic surface with abundant hierarchical roughness would lead to the decrease in the air fraction of solid/liquid interfaces beneath the water droplet by reducing the actual contact area of the water droplet on the surface structures, as stated previously. Additionally, all of these samples were endowed with excellent superoleophilicity with the extremely low OCA of  $0^\circ$ , which was attributed to the long alkyl chain of RSH with a low surface energy and the capillary effect.<sup>16</sup> Thus, this promising selective wettability could make the nanofibrous membranes good candidates for oil/water separation.

The rolling-off properties of the water droplet placed on the fabricated membranes were examined by measuring the water contact angle hysteresis (WCAH), which was based on the increment–decrement method. As shown in Figure 3B, the WCAHs decreased obviously with the increasing electroless plating time, and the lowest value of  $3.0 \pm 0.6^\circ$  from the as-prepared APAN-Ag-SR-60 surface indicated  $\sim 7$ -fold enhancement compared to that of the APAN-Ag-SR-30 ( $22.0 \pm 0.7^\circ$ ), which was in accordance with the WCAs tested. Further study of the rolling-off properties of the APAN-Ag-SR-50 was conducted by observing the sliding behavior of a water droplet (controlled by a microneedle to be about  $10 \mu\text{L}$ ) on a dry membrane surface and an oil (EDB) wetted surface that tilted with a very low angle ( $\alpha$ ) of  $5^\circ$ . Figure 4 represents the time-sequential photograph images of a moving water droplet indicated by a white dotted-arrow, which exhibited a highly water-repellent property. It was observed that the water droplets rolled off immediately over the tilted surface and disappeared within 252 ms, even for the oil wetted membrane surface (see the Supporting Information, Video 1). In addition, Figure 3C shows the photographs of the dynamic water-adhesion behavior on the APAN-Ag-SR-50 surface within 2 s. As can be seen, a water droplet contacted with the surface could leave it with extremely low adhesion after the needle preloading. Consequently, these antiwetting properties indicated that the as-prepared superhydrophobic membranes are suitable for a range of applications that require a self-cleaning surface.

**Structural Stability.** Liquid entry pressure of water (LEPw, sometimes faulty called “wetting pressure”) is the pressure that must be applied onto deionized water before it penetrates into a nonwetted (dry) membrane,<sup>39</sup> i.e., water droplet cannot pass

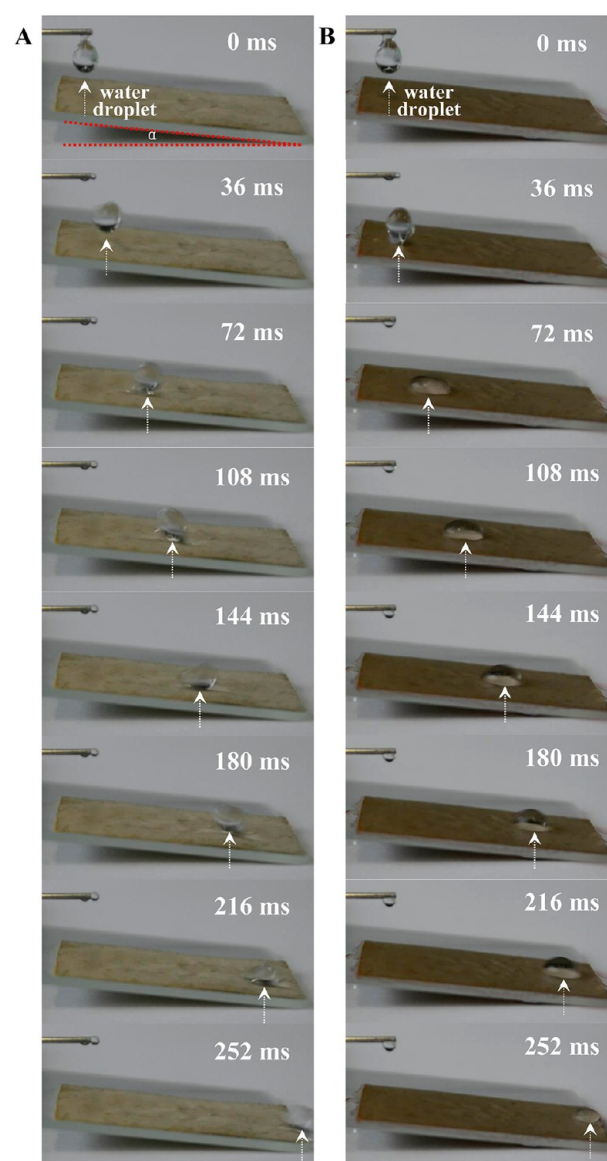


**Figure 4.** Sequential photographic images of  $10 \mu\text{L}$  water droplets on a dry APAN-Ag-SR-50 membrane surface (A) and an oil (EDB) wetted surface (B) that tilted with a very low angle ( $\alpha$ ) of  $5^\circ$ .

through the membrane below this breakthrough pressure. Figure 5A shows the schematic diagram of the superhydrophobic membrane pores wetting process under LEPw. The spherical water droplets located on the hierarchically rough surface were compelled to permeate into the membrane pores and induced the occurrence of wetting, then resulted in the elimination of superhydrophobicity, which was subjected to LEPw. Thus, the separation capability of the fabricated membranes could be evaluated by measuring the LEPw. As shown in Figure 5B, with the increasing of electroless plating time from 30 to 60 min, the obtained LEPw values of the samples were  $50 \pm 6$ ,  $115 \pm 2$ ,  $170 \pm 4$  and  $175 \pm 3$  kPa, respectively. It is noteworthy that the maximum LEPw of APAN-Ag-SR-60 was approximate to the conventional PVDF commercial membrane fabricated by phase inversion ( $120$ – $291$  kPa from different membrane pore sizes),<sup>45,46</sup> which provided the basic structural prerequisite for oil/water separation.

The robustness of the immobilized Ag nanocluster was tested by ultrasonication in ethanol for 30 min. The representative FE-

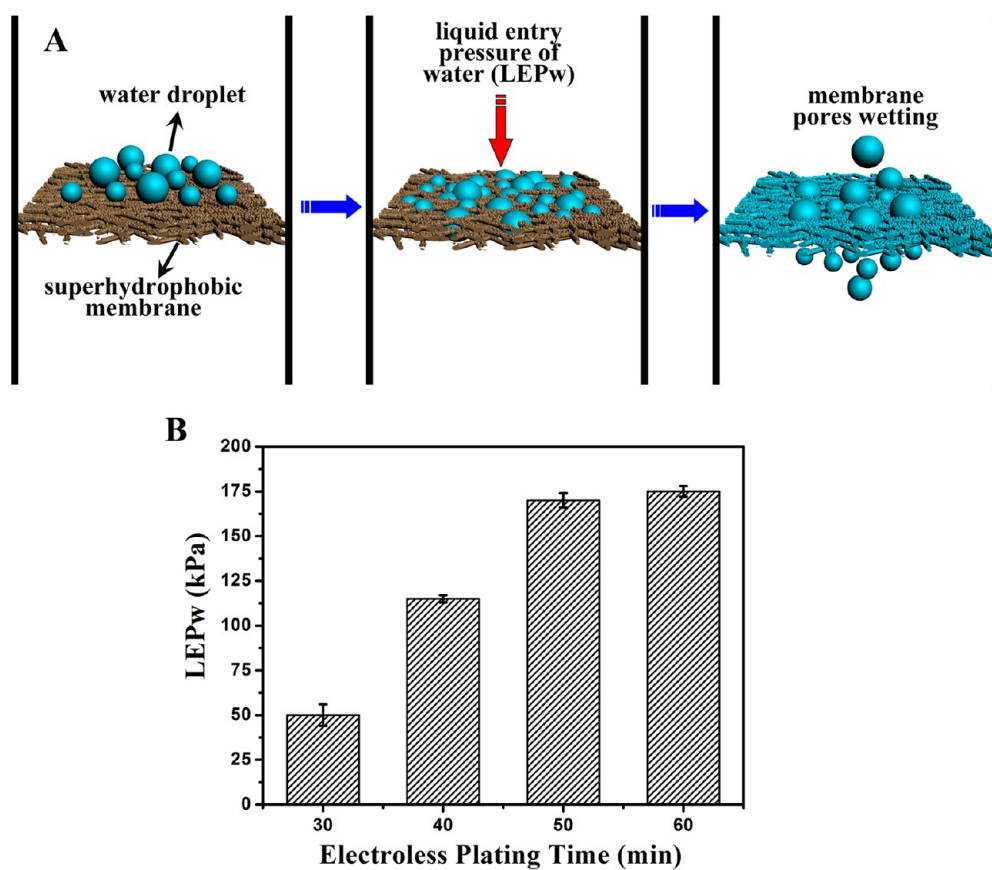


**Figure 5.** (A) Schematic diagram of the superhydrophobic membrane pores wetting under liquid entry pressure of water (LEPw). (B) LEPw values of the resultant membranes with different electroless plating time.

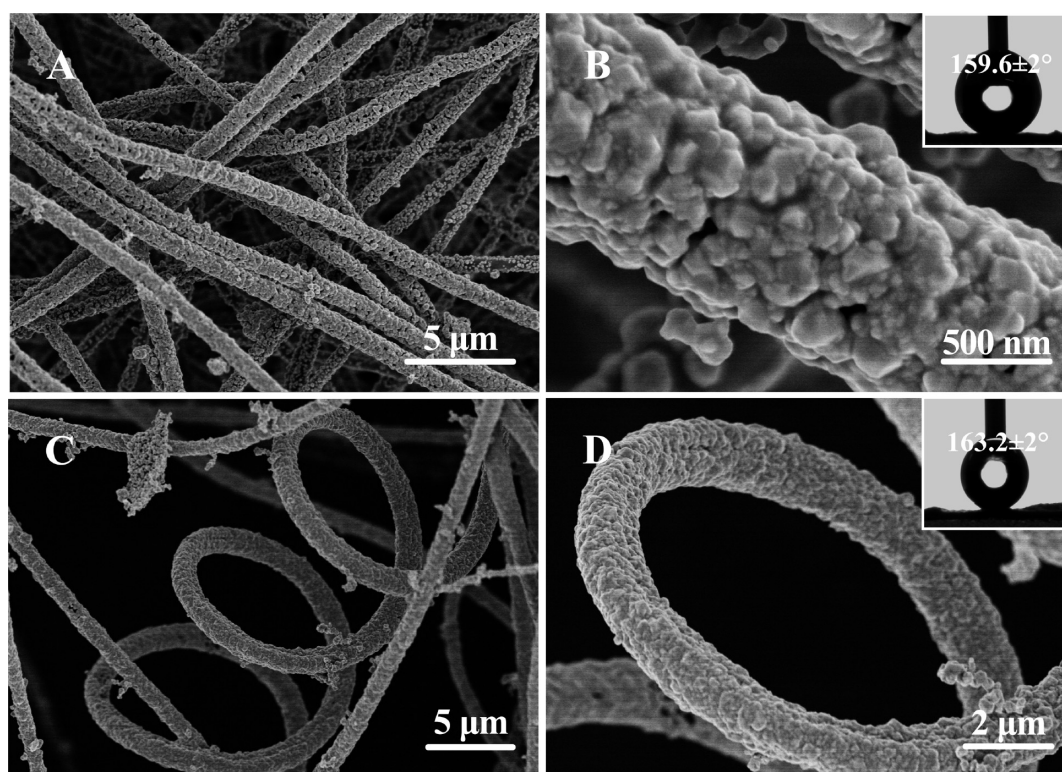
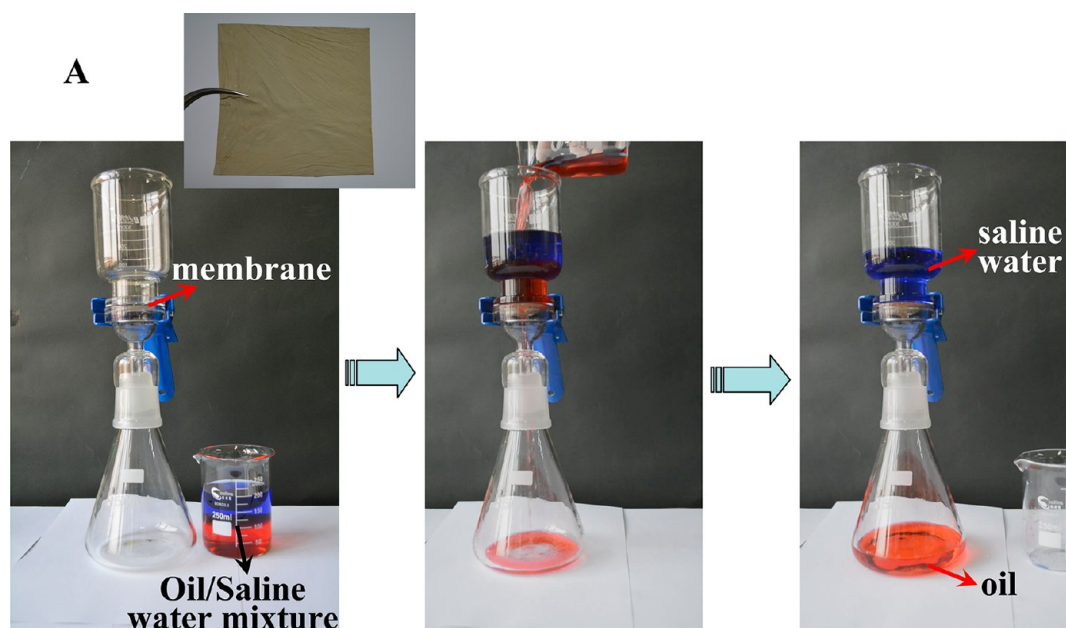


**Figure 6.** FE-SEM images of the APAN-Ag-SR-50 nanofibrous membranes after ultrasonication in ethanol for 30 min (A, B), and fiber morphology after peeling off the membrane surface layer (C, D). The insets in panels B and D are the water contact angles.





### Fast separation for 1 min

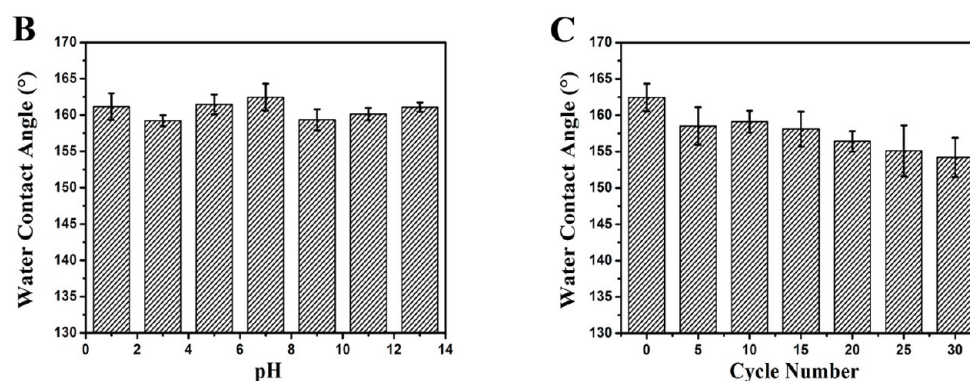


**Figure 7.** (A) Oil/water separation studies of the APAN-Ag-SR-50 membranes. For clarity, the saline water and oil were dyed by methyl blue and Sudan III, respectively. (B) Relationship between pH and the WCAs of APAN-Ag-SR-50 membranes. (C) WCAs recorded for the APAN-Ag-SR-50 membranes after each oil/water separation process.

SEM observations of as-prepared APAN-Ag-SR-50 shown in Figure 6A,B demonstrated that Ag nanoclusters anchored on the APAN nanofibers surfaces were able to withstand ultrasonication without significant decrease in coverage, which was ascribed to the sufficient chemi-sorption sites from the abundant amine and imine groups. Meanwhile, the sample surface still exhibited a superhydrophobic property with a WCA of  $159.6 \pm 2^\circ$ . Additionally, the surface layer of APAN-Ag-SR-50 was peeled off to get a further observation of the inner immobilization state. Interestingly, a helically self-crimped fiber morphology was discovered, as shown in Figure 6C,D, probably attributed to the uneven stretching force acting on the fiber or occurred spontaneously on removal of the drawing tension during the peeling process,<sup>47</sup> which is similar to the self-crimped hair after uneven stressing. More importantly, these unique robust fiber morphologies well confirmed the excellent immobilization of Ag nanocluster on the APAN surfaces. Similarly, the inner surface displayed superhydrophobicity with a WCA of  $163.2 \pm 2^\circ$ .

**Gravity Driven Oil/Water Separation.** Considering the complex practical environments of seawater and industry, it is of vital importance to investigate the separation capability and stability of the as-prepared membranes with unique selective wettability for oil/water separation. Thus, a series of proof-of-concept studies were carried out to test the solely gravity driven oil/water separation capability of the APAN-Ag-SR-50 membranes. As shown in Figure 7A, the membrane with a thickness of  $100 \mu\text{m}$  was fixed between the glass funnel and conical flask, and a 200 mL saline mixture of a heavier oil (1,2-dibromoethane (EDB), 50% v/v) and water (35 g/L NaCl solution) was poured onto the sample surface. Oil quickly permeated through the membranes and dropped into the conical flask due to the superoleophilicity. Meanwhile, the saline water was repelled and retained above the membranes due to the superhydrophobicity and low water-adhesion property of the membranes. No external force was employed during the fast separation process (within 60 s and a fascinating permeate flux of  $4774.6 \pm 45.6 \text{ L}\cdot\text{m}^{-2}\cdot\text{h}^{-1}$ ); only gravity was responsible for the separation (see the Supporting Information,



Video 2), indicating its ease of operation and low energy consumption. Also, no colored saline water in the collected oil or oil in the collected saline water was detected, which indicated a very high separation efficiency of the APAN-Ag-SR-50 membranes and a stable separation capacity in a hyper-saline environment. It is noteworthy that the membrane thickness will play an important role in permeate flux during the separation process. While even though the membrane thickness was increased to 250  $\mu\text{m}$ , it still exhibited a very high permeate flux ( $1061.1 \pm 38.2 \text{ L}\cdot\text{m}^{-2}\cdot\text{h}^{-1}$ , see the Supporting Information, Figure S5).

In addition, the stability in acidic and alkaline environments of the practical oil/water separation were also investigated, as shown in Figure 7B, the APAN-Ag-SR-50 membranes exhibited robust superhydrophobicity toward water with a broad range of pH. And the oil/water separation of the mixture with pH controlled at 1 and 11 both exhibited excellent separation efficiency (see the Supporting Information, Figure S6), indicating the certain stability against corrosive conditions. Moreover, Figure 7C recorded the WCAs of the APAN-Ag-SR-50 membranes after each separation process, which still exhibited a WCA larger than  $150^\circ$  after separating oil for 30 cycles, showing the excellent recyclability. On the other hand, the APAN-Ag-SR-50 nanofibrous membrane could still possess excellent separation efficiency for a variety of oil/water mixtures including chloroform, *n*-hexane, petroleum ether, vegetable oil, vacuum pump oil, etc. The permeate flux of the membrane with different mixtures was performed as shown in Figure 8, which

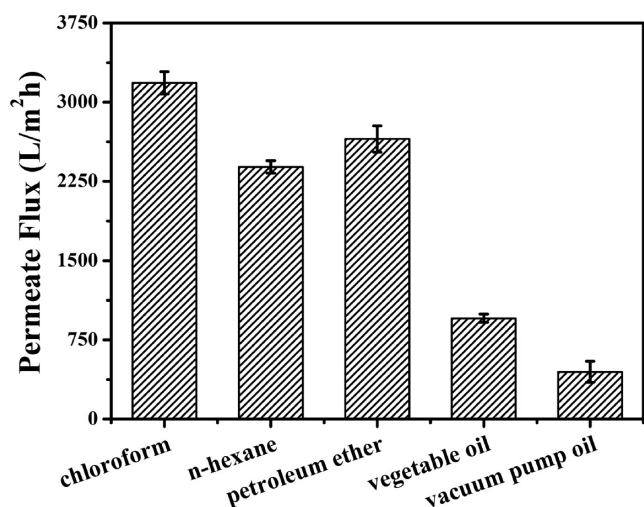


**Figure 8.** Permeate flux of the APAN-Ag-SR-50 nanofibrous membrane with a thickness of 100  $\mu\text{m}$  for the separation of different oil/water mixtures.

demonstrated that the membrane could possess fascinating permeate fluxes for the low-viscosity oils, and relatively lower values for the high-viscosity oils ( $954.9 \pm 38.5 \text{ L}\cdot\text{m}^{-2}\cdot\text{h}^{-1}$  for vegetable oil and  $447.5 \pm 100.3 \text{ L}\cdot\text{m}^{-2}\cdot\text{h}^{-1}$  for vacuum pump oil) due to the intrinsic oleophilicity of the sample. In this case, as compared to those superhydrophilic and underwater superoleophobic materials,<sup>48–50</sup> the APAN-Ag-SR-50 nanofibrous membrane exhibited relatively undistinguished results, while the membrane still could be easily cleaned by ethanol for reuse after the separation of high-viscosity oil/water mixtures. Consequently, the above obtained results suggest that the as-prepared APAN-Ag-SR-50 membranes are promising candi-

dates for industrial oil-contaminated water treatments and marine spilt oil cleanup, especially from a practical point of view.

## CONCLUSIONS

In summary, a novel superhydrophobic and superoleophilic nanofibrous membrane with excellent oil/water separation performance was successfully fabricated by a facile combination of APAN nanofibers and immobilization of Ag nanoclusters, followed by modification with long alkyl chain thiols. The fine hierarchical roughness constructed on APAN nanofibers surfaces could be regulated by tuning the electroless plating time. The resultant APAN-Ag-SR-50 membranes showed a high WCA of  $162.4 \pm 1.9^\circ$ , an extremely low OCA of  $0^\circ$  and a self-cleaning surface with WCAH of  $3.4 \pm 0.9^\circ$  and low water-adhesion property. Significantly, the as-prepared APAN-Ag-SR-50 membranes with high LEPw and robust fiber morphology exhibited fast and efficient separation for oil/water mixture in both hyper-saline environment and broad pH range conditions, as well as excellent recyclability, suggesting their use as promising separators for industrial oil-contaminated water treatment and marine spilt oil cleanup.

## ASSOCIATED CONTENT

### Supporting Information

Proposed amination mechanism of the DETA grafted on the PAN nanofibers, apparatus for the determination of the LEPw, XPS N 1s spectra for the PAN and APAN nanofibrous membranes, FE-SEM images of APAN-Ag-SR-x membranes with the prolonged electroless plating time from 70 to 100 min, XPS results of the APAN-Ag and APAN-Ag-SR membranes surfaces, the relationship between the permeate flux and membrane thickness of APAN-Ag-SR-50 nanofibrous membranes during the oil (EDB)/saline water separation process, photographs of oil/acid solution (pH = 1) separation and oil/alkali solution (pH = 11) separation of the APAN-Ag-SR-50 membranes, atom content of the PAN and APAN membranes, the porosity of the as-prepared APAN-Ag-SR-x nanofibrous membranes, video of the water droplets rolling off over a dry APAN-Ag-SR-50 membrane surface and an oil wetted surface that tilted with a very low angle of  $5^\circ$  and video of oil/water separation process of APAN-Ag-SR-50 membranes in a hyper-saline environment. This material is available free of charge via the Internet at <http://pubs.acs.org>.

## AUTHOR INFORMATION

### Corresponding Author

\*X. Wang. Tel.: +86-21-67792860. Fax: +86-21-67792855. E-mail: wangxf@dhu.edu.cn.

### Notes

The authors declare no competing financial interest.

## ACKNOWLEDGMENTS

This work was supported by National Science Foundation of China (51273042, 21174028), Program for New Century Excellent Talents in University, Innovation Program of Shanghai Municipal Education Commission, Program of Changjiang Scholars and Innovative Research Team in University (IRT1221) and National 863 Program of China (2012AA030309).

## ■ REFERENCES

- (1) Jernelöv, A. How to Defend against Future Oil Spills. *Nature* **2010**, *466*, 182–183.
- (2) Shannon, M. A.; Bohn, P. W.; Elimelech, M.; Georgiadis, J. G.; Mariñas, B. J.; Mayes, A. M. Science and Technology for Water Purification in the Coming Decades. *Nature* **2008**, *452*, 301–310.
- (3) Adebajo, M. O.; Frost, R. L.; Klopogge, J. T.; Carmody, O.; Kokot, S. Porous Materials for Oil Spill Cleanup: A Review of Synthesis and Absorbing Properties. *J. Porous. Mater.* **2003**, *10*, 159–170.
- (4) Kota, A. K.; Kwon, G.; Choi, W.; Mabry, J. M.; Tuteja, A. Hygro-Responsive Membranes for Effective Oil–Water Separation. *Nat. Commun.* **2012**, *3*, 1025.
- (5) Yuan, J.; Liu, X.; Akbulut, O.; Hu, J.; Suib, S. L.; Kong, J.; Stellacci, F. Superwetting Nanowire Membranes for Selective Absorption. *Nat. Nanotechnol.* **2008**, *3*, 332–336.
- (6) Zhang, L.; Zhang, Z.; Wang, P. Smart Surfaces with Switchable Superoleophilicity and Superoleophobicity in Aqueous Media: Toward Controllable Oil/Water Separation. *NPG Asia Mater.* **2012**, *4*, e8.
- (7) Wang, X.; Chen, X.; Yoon, K.; Fang, D.; Hsiao, B. S.; Chu, B. High Flux Filtration Medium Based on Nanofibrous Substrate with Hydrophilic Nanocomposite Coating. *Environ. Sci. Technol.* **2005**, *39*, 7684–7691.
- (8) Cheryan, M.; Rajagopalan, N. Membrane Processing of Oily Streams. Wastewater Treatment and Waste Reduction. *J. Membr. Sci.* **1998**, *151*, 13–28.
- (9) El-Kayar, A.; Hussein, M.; Zatout, A.; Hosny, A.; Amer, A. Removal of Oil from Stable Oil–Water Emulsion by Induced Air Flotation Technique. *Sep. Technol.* **1993**, *3*, 25–31.
- (10) Hosny, A. Y. Separating Oil from Oil–Water Emulsions by Electroflotation Technique. *Sep. Technol.* **1996**, *6*, 9–17.
- (11) Liu, M.; Zheng, Y.; Zhai, J.; Jiang, L. Bioinspired Super-Antiwetting Interfaces with Special Liquid–Solid Adhesion. *Acc. Chem. Res.* **2009**, *43*, 368–377.
- (12) Levkin, P. A.; Svec, F.; Fréchet, J. M. Porous Polymer Coatings: A Versatile Approach to Superhydrophobic Surfaces. *Adv. Funct. Mater.* **2009**, *19*, 1993–1998.
- (13) Yao, X.; Song, Y.; Jiang, L. Applications of Bio-Inspired Special Wettable Surfaces. *Adv. Mater.* **2011**, *23*, 719–734.
- (14) Wenzel, R. N. Resistance of Solid Surfaces to Wetting by Water. *Ind. Eng. Chem.* **1936**, *28*, 988–994.
- (15) Cassie, A.; Baxter, S. Wettability of Porous Surfaces. *Trans. Faraday Soc.* **1944**, *40*, 546–551.
- (16) Feng, X.; Jiang, L. Design and Creation of Superwetting/Antiwetting Surfaces. *Adv. Mater.* **2006**, *18*, 3063–3078.
- (17) Lafuma, A.; Quere, D. Superhydrophobic States. *Nat. Mater.* **2003**, *2*, 457–60.
- (18) Feng, L.; Zhang, Z.; Mai, Z.; Ma, Y.; Liu, B.; Jiang, L.; Zhu, D. A Super-Hydrophobic and Super-Oleophilic Coating Mesh Film for the Separation of Oil and Water. *Angew. Chem., Int. Ed.* **2004**, *43*, 2012–2014.
- (19) Wang, C.; Yao, T.; Wu, J.; Ma, C.; Fan, Z.; Wang, Z.; Cheng, Y.; Lin, Q.; Yang, B. Facile Approach in Fabricating Superhydrophobic and Superoleophilic Surface for Water and Oil Mixture Separation. *ACS Appl. Mater. Interfaces* **2009**, *1*, 2613–2617.
- (20) Zhang, J.; Seeger, S. Polyester Materials with Superwetting Silicone Nanofilaments for Oil/Water Separation and Selective Oil Absorption. *Adv. Funct. Mater.* **2011**, *21*, 4699–4704.
- (21) Shiu, J.-Y.; Kuo, C.-W.; Chen, P.; Mou, C.-Y. Fabrication of Tunable Superhydrophobic Surfaces by Nanosphere Lithography. *Chem. Mater.* **2004**, *16*, 561–564.
- (22) Song, X.; Zhai, J.; Wang, Y.; Jiang, L. Fabrication of Superhydrophobic Surfaces by Self-Assembly and Their Water-Adhesion Properties. *J. Phys. Chem. B* **2005**, *109*, 4048–4052.
- (23) Wu, X.; Shi, G. Production and Characterization of Stable Superhydrophobic Surfaces Based on Copper Hydroxide Nanoneedles Mimicking the Legs of Water Striders. *J. Phys. Chem. B* **2006**, *110*, 11247–11252.
- (24) Tserepi, A.; Vlachopoulou, M.; Gogolides, E. Nanotexturing of Poly (Dimethylsiloxane) in Plasmas for Creating Robust Super-Hydrophobic Surfaces. *Nanotechnology* **2006**, *17*, 3977.
- (25) Dzenis, Y. Spinning Continuous Fibers for Nanotechnology. *Science* **2004**, *304*, 1917–1919.
- (26) Tuteja, A.; Choi, W.; Ma, M.; Mabry, J. M.; Mazzella, S. A.; Rutledge, G. C.; McKinley, G. H.; Cohen, R. E. Designing Superoleophobic Surfaces. *Science* **2007**, *318*, 1618–1622.
- (27) Ma, M.; Gupta, M.; Li, Z.; Zhai, L.; Gleason, K. K.; Cohen, R. E.; Rubner, M. F.; Rutledge, G. C. Decorated Electrospun Fibers Exhibiting Superhydrophobicity. *Adv. Mater.* **2007**, *19*, 255–259.
- (28) Wang, X.; Ding, B.; Yu, J.; Wang, M. Engineering Biomimetic Superhydrophobic Surfaces of Electrospun Nanomaterials. *Nano Today* **2011**, *6*, 510–530.
- (29) Zhu, H.; Qiu, S.; Jiang, W.; Wu, D.; Zhang, C. Evaluation of Electrospun Polyvinyl Chloride/Polystyrene Fibers as Sorbent Materials for Oil Spill Cleanup. *Environ. Sci. Technol.* **2011**, *45*, 4527–4531.
- (30) Lin, J.; Ding, B.; Yang, J.; Yu, J.; Sun, G. Subtle Regulation of the Micro- and Nanostructures of Electrospun Polystyrene Fibers and Their Application in Oil Absorption. *Nanoscale* **2012**, *4*, 176–182.
- (31) Wu, J.; Wang, N.; Wang, L.; Dong, H.; Zhao, Y.; Jiang, L. Electrospun Porous Structure Fibrous Film with High Oil Adsorption Capacity. *ACS Appl. Mater. Interfaces* **2012**, *4*, 3207–3212.
- (32) Shang, Y.; Si, Y.; Raza, A.; Yang, L.; Mao, X.; Ding, B.; Yu, J. An In Situ Polymerization Approach for the Synthesis of Superhydrophobic and Superoleophilic Nanofibrous Membranes for Oil–Water Separation. *Nanoscale* **2012**, *4*, 7847–7854.
- (33) Tang, X.; Si, Y.; Ge, J.; Ding, B.; Liu, L.; Zheng, G.; Luo, W.; Yu, J. In Situ Polymerized Superhydrophobic and Superoleophilic Nanofibrous Membranes for Gravity Driven Oil–Water Separation. *Nanoscale* **2013**, *5*, 11657–11664.
- (34) Fu, Y.; Liu, L.; Zhang, L.; Wang, W. Highly Conductive One-Dimensional Nanofibers: Silvered Electrospun Silica Nanofibers via Poly(dopamine) Functionalization. *ACS Appl. Mater. Interfaces* **2014**, *6*, 5105–5112.
- (35) Zhu, Q.; Pan, Q. Mussel-Inspired Direct Immobilization of Nanoparticles and Application for Oil–Water Separation. *ACS Nano* **2014**, *8*, 1402–1409.
- (36) Zhang, L.; Wu, J.; Wang, Y.; Long, Y.; Zhao, N.; Xu, J. Combination of Bioinspiration: A General Route to Superhydrophobic Particles. *J. Am. Chem. Soc.* **2012**, *134*, 9879–9881.
- (37) Wang, W.; Jiang, Y.; Liao, Y.; Tian, M.; Zou, H.; Zhang, L. Fabrication of Silver-Coated Silica Microspheres through Mussel-Inspired Surface Functionalization. *J. Colloid Interface Sci.* **2011**, *358*, 567–574.
- (38) Neghlani, P. K.; Rafizadeh, M.; Taromi, F. A. Preparation of Aminated-Polyacrylonitrile Nanofiber Membranes for the Adsorption of Metal Ions: Comparison with Microfibers. *J. Hazard. Mater.* **2011**, *186*, 182–189.
- (39) Smolders, K.; Franken, A. C. M. Terminology for Membrane Distillation. *Desalination* **1989**, *72*, 249–262.
- (40) Li, X.; Wang, C.; Yang, Y.; Wang, X.; Zhu, M.; Hsiao, B. S. Dual-Biomimetic Superhydrophobic Electrospun Polystyrene Nanofibrous Membranes for Membrane Distillation. *ACS Appl. Mater. Interfaces* **2014**, *6*, 2423–30.
- (41) Deng, S.; Bai, R. Adsorption and Desorption of Humic Acid on Aminated Polyacrylonitrile Fibers. *J. Colloid Interface Sci.* **2004**, *280*, 36–43.
- (42) Deng, S.; Bai, R.; Chen, J. P. Aminated Polyacrylonitrile Fibers for Lead and Copper Removal. *Langmuir* **2003**, *19*, 5058–5064.
- (43) Deng, S.; Bai, R. B. Aminated Polyacrylonitrile Fibers for Humic Acid Adsorption: Behaviors and Mechanisms. *Environ. Sci. Technol.* **2003**, *37*, 5799–5805.
- (44) Laibinis, P. E.; Whitesides, G. M.; Allara, D. L.; Tao, Y. T.; Parikh, A. N.; Nuzzo, R. G. Comparison of the Structures and Wetting Properties of Self-Assembled Monolayers of N-Alkanethiols on the Coinage Metal Surfaces, Copper, Silver, and Gold. *J. Am. Chem. Soc.* **1991**, *113*, 7152–7167.



(45) Lalia, B. S.; Guillen-Burrieza, E.; Arafat, H. A.; Hashaikh, R. Fabrication and Characterization of Polyvinylidene fluoride-Co-Hexafluoropropylene (Pvdf-Hfp) Electrospun Membranes for Direct Contact Membrane Distillation. *J. Membr. Sci.* **2013**, *428*, 104–115.

(46) Razmjou, A.; Arifin, E.; Dong, G.; Mansouri, J.; Chen, V. Superhydrophobic Modification of TiO<sub>2</sub> Nanocomposite PVDF Membranes for Applications in Membrane Distillation. *J. Membr. Sci.* **2012**, *415*, 850–863.

(47) Lin, T.; Wang, H.; Wang, X. Self-Crimping Bicomponent Nanofibers Electrospun from Polyacrylonitrile and Elastomeric Polyurethane. *Adv. Mater.* **2005**, *17*, 2699–2703.

(48) Chen, Y.; Xue, Z.; Liu, N.; Lu, F.; Cao, Y.; Sun, Z.; Feng, L. Fabrication of a Silica Gel Coated Quartz Fiber Mesh for Oil–Water Separation under Strong Acidic and Concentrated Salt Conditions. *RSC Adv.* **2014**, *4*, 11447–11450.

(49) Gao, C.; Sun, Z.; Li, K.; Chen, Y.; Cao, Y.; Zhang, S.; Feng, L. Integrated Oil Separation and Water Purification by a Double-Layer TiO<sub>2</sub>-based Mesh. *Energy Environ. Sci.* **2013**, *6*, 1147–1151.

(50) Zhang, S.; Lu, F.; Tao, L.; Liu, N.; Gao, C.; Feng, L.; Wei, Y. Bio-Inspired Anti-Oil-Fouling Chitosan-Coated Mesh for Oil/Water Separation Suitable for Broad pH Range and Hyper-Saline Environments. *ACS Appl. Mater. Interfaces* **2013**, *5*, 11971–11976.